Measurement of y_{CP} in D^0 meson decays to the $K^0_S K^+ K^-$ final state

A. Zupanc,[14] I. Adachi,[8] H. Aihara,[44] K. Arinstein,[1,31] V. Aulchenko,[1,31] T. Aushev,[18,13] A. M. Bakich,[39] V. Balagura,[13] E. Barberio,[21] A. Bay,[18] K. Belous,[12] M. Bischofberger,[23] A. Bozek,[27] M. Bračko,[20,14] J. Brodzicka,[8] T. E. Browder,[7] M.-C. Chang,[4] Y. Chao,[26] A. Chen,[24] B. G. Cheon,[6] C.-C. Chiang,[26] I.-S. Cho,[48] Y. Choi,[38] J. Dalseno,[8] A. Drutskoy,[2] W. Dungel,[11] S. Eidelman,[1,31] N. Gabyshev,[1,31] P. Goldenzweig,[2] B. Golob,[19,14] H. Ha,[16] J. Haba,[8] B.-Y. Han,[16] T. Hara,[8] Y. Hasegawa,[37] K. Hayasaka,[22] H. Hayashii,[23] M. Hazumi,[8] Y. Hoshi,[42] H. J. Hyun,[17] K. Inami,[22] A. Ishikawa,[34] R. Itoh,[8] M. Iwasaki,[44] N. J. Joshi,[40] D. H. Kah,[17] J. H. Kang,[48] P. Kapusta,[27] N. Katayama,[8] T. Kawasaki,[29] H. O. Kim,[17] Y. I. Kim,[17] Y. J. Kim,[5] K. Kinoshita,[2] B. R. Ko,[16] S. Korpar,[20,14] P. Križan,[19,14] P. Krokovny,[8] R. Kumar,[33] Y.-J. Kwon,[48] S.-H. Kyeong,[48] M. J. Lee,[36] T. Lesiak,[27,3] J. Li,[7] C. Liu,[35] Y. Liu,[22] R. Louvot,[18] A. Matyja,[27] S. McOnie,[39] K. Miyabayashi,[23] H. Miyata,[29] Y. Miyazaki,[22] R. Mizuk,[13] Y. Nagasaka,[9] E. Nakano,[32] M. Nakao,[8] Z. Natkaniec,[27] S. Nishida,[8] K. Nishimura,[7] O. Nitoh,[46] S. Ogawa,[41] T. Ohshima,[22] S. Okuno,[15] H. Ozaki,[8] P. Pakhlov,[13] G. Pakhlova,[13] C. W. Park,[38] H. Park,[17] H. K. Park,[17] R. Pestotnik,[14] L. E. Piilonen,[47] A. Poluektov,[1,31] H. Sahoo,[7] K. Sakai,[29] Y. Sakai,[8] O. Schneider,[18] A. J. Schwartz,[2] A. Sekiya,[23] K. Senyo,[22] M. E. Sevior,[21] M. Shapkin,[12] C. P. Shen,[7] J.-G. Shiu,[26] B. Shwartz,[1,31] J. B. Singh,[33] A. Sokolov,[12] S. Stanič,[30] M. Starič,[14] T. Sumiyoshi,[45] G. N. Taylor,[21] Y. Teramoto,[32] K. Trabelsi,[8] S. Uehara,[8] Y. Unno,[6] S. Uno,[8] P. Urquijo,[21] Y. Usov,[1,31] G. Varner,[7] K. E. Varvell,[39] K. Vervink,[18] A. Vinokurova,[1,31] C. H. Wang,[25] M.-Z. Wang,[26] P. Wang,[10] Y. Watanabe,[15] R. Wedd,[21] E. Won,[16] B. D. Yabsley,[39] H. Yamamoto,[43] Y. Yamashita,[28] Z. P. Zhang,[35] V. Zhilich,[1,31] V. Zhulanov,[1,31] T. Zivko,[14] and O. Zyukova[1,31]

(The Belle Collaboration)

[1]*Budker Institute of Nuclear Physics, Novosibirsk*
[2]*University of Cincinnati, Cincinnati, Ohio 45221*
[3]*T. Kościuszko Cracow University of Technology, Krakow*
[4]*Department of Physics, Fu Jen Catholic University, Taipei*
[5]*The Graduate University for Advanced Studies, Hayama*
[6]*Hanyang University, Seoul*
[7]*University of Hawaii, Honolulu, Hawaii 96822*
[8]*High Energy Accelerator Research Organization (KEK), Tsukuba*
[9]*Hiroshima Institute of Technology, Hiroshima*
[10]*Institute of High Energy Physics, Chinese Academy of Sciences, Beijing*
[11]*Institute of High Energy Physics, Vienna*
[12]*Institute of High Energy Physics, Protvino*
[13]*Institute for Theoretical and Experimental Physics, Moscow*
[14]*J. Stefan Institute, Ljubljana*
[15]*Kanagawa University, Yokohama*
[16]*Korea University, Seoul*
[17]*Kyungpook National University, Taegu*
[18]*École Polytechnique Fédérale de Lausanne (EPFL), Lausanne*
[19]*Faculty of Mathematics and Physics, University of Ljubljana, Ljubljana*
[20]*University of Maribor, Maribor*
[21]*University of Melbourne, School of Physics, Victoria 3010*
[22]*Nagoya University, Nagoya*
[23]*Nara Women's University, Nara*
[24]*National Central University, Chung-li*
[25]*National United University, Miao Li*
[26]*Department of Physics, National Taiwan University, Taipei*
[27]*H. Niewodniczanski Institute of Nuclear Physics, Krakow*
[28]*Nippon Dental University, Niigata*
[29]*Niigata University, Niigata*
[30]*University of Nova Gorica, Nova Gorica*
[31]*Novosibirsk State University, Novosibirsk*
[32]*Osaka City University, Osaka*
[33]*Panjab University, Chandigarh*
[34]*Saga University, Saga*
[35]*University of Science and Technology of China, Hefei*
[36]*Seoul National University, Seoul*

[37]*Shinshu University, Nagano*
[38]*Sungkyunkwan University, Suwon*
[39]*University of Sydney, Sydney, New South Wales*
[40]*Tata Institute of Fundamental Research, Mumbai*
[41]*Toho University, Funabashi*
[42]*Tohoku Gakuin University, Tagajo*
[43]*Tohoku University, Sendai*
[44]*Department of Physics, University of Tokyo, Tokyo*
[45]*Tokyo Metropolitan University, Tokyo*
[46]*Tokyo University of Agriculture and Technology, Tokyo*
[47]*IPNAS, Virginia Polytechnic Institute and State University, Blacksburg, Virginia 24061*
[48]*Yonsei University, Seoul*
(Received 26 May 2009; published 18 September 2009)

We present a measurement of the $D^0 - \bar{D}^0$ mixing parameter y_{CP} using a flavor-untagged sample of $D^0 \to K^0_S K^+ K^-$ decays. The measurement is based on a 673 fb^{-1} data sample recorded with the Belle detector at the KEKB asymmetric-energy e^+e^- collider. Using a method based on measuring the mean decay time for different K^+K^- invariant mass intervals, we find $y_{CP} = (+0.11 \pm 0.61(\text{stat.}) \pm 0.52(\text{syst.}))\%$.

DOI: 10.1103/PhysRevD.80.052006 PACS numbers: 13.25.Ft, 12.15.Ff

I. INTRODUCTION

Particle-antiparticle mixing has been observed in the neutral kaon, B^0_d and B^0_s meson systems, and evidence for mixing has recently been found for neutral D mesons. The mixing occurs through weak interactions and gives rise to two distinct mass eigenstates: $|D_{1,2}\rangle = p|D^0\rangle \pm q|\bar{D}^0\rangle$, where p and q are complex coefficients satisfying $|p|^2 + |q|^2 = 1$. The time evolution of the flavor eigenstates, D^0 and $\bar{D}^0$, is governed by the mixing parameters $x = (m_1 - m_2)/\Gamma$ and $y = (\Gamma_1 - \Gamma_2)/2\Gamma$, where $m_{1,2}$ and $\Gamma_{1,2}$ are the masses and widths of the two mass eigenstates $D_{1,2}$ and $\Gamma = (\Gamma_1 + \Gamma_2)/2$. In the standard model (SM) the contribution of the box diagram, successfully describing mixing in the B- and K-meson systems, is strongly suppressed for D^0 mesons due both to the smallness of the V_{ub} element of the Cabibbo-Kobayashi-Maskawa matrix [1], and to the Glashow-Illiopoulos-Maiani mechanism [2]. The largest SM predictions for the parameters x and y, which include the impact of long distance dynamics, are of order 1% [3]. Observation of large mixing could indicate the contribution of new processes and particles.

Evidence for $D^0 - \bar{D}^0$ mixing has been found in $D^0 \to K^+K^-/\pi^+\pi^-$ [4,5], $D^0 \to K^+\pi^-$ [6,7] and $D^0 \to K^+\pi^-\pi^0$ [8] decays. Currently the most precise individual measurements of mixing parameters are those from the relative lifetime difference between D^0 decays to CP eigenstates and flavor-specific final states, y_{CP}, which equals the parameter y in the limit where CP is conserved. Thus far, only CP-even final states K^+K^- and $\pi^+\pi^-$ have been used; the resulting world average value [9] for y_{CP} is $(+1.13 \pm 0.27)\%$.

In this paper we present a flavor-untagged measurement of y_{CP} using the CP-odd component of $D^0 \to K^0_S K^+ K^-$ decays [10]. The measurement is performed by comparing mean decay times for different regions of the three-body phase space distribution. As this method does not use a fit to the decay-time distribution, it does not require detailed knowledge of the resolution function or the time distribution of backgrounds. The result has similar statistical sensitivity to that obtained by fitting the decay-time distribution.

II. METHOD

The time-dependent decay amplitude of an initially produced D^0 or $\bar{D}^0$ can be expressed in terms of the neutral D meson amplitudes $\langle K^0_S K^+ K^-|D^0\rangle = \mathcal{A}(s_0, s_+)$ and $\langle K^0_S K^+ K^-|\bar{D}^0\rangle = \bar{\mathcal{A}}(s_0, s_+)$, where $s_0 = M^2_{K^+K^-}$ [11] and $s_\pm = M^2_{K^0_S K^\pm}$. The explicit expressions are [12,13]

$$\langle K^0_S K^+ K^-|D^0(t)\rangle = \frac{1}{2}\left[\mathcal{A}(s_0, s_+) + \frac{q}{p}\bar{\mathcal{A}}(s_0, s_+)\right]e_1(t) + \frac{1}{2}\left[\mathcal{A}(s_0, s_+) - \frac{q}{p}\bar{\mathcal{A}}(s_0, s_+)\right]e_2(t) \tag{1}$$

$$\langle K^0_S K^+ K^-|\bar{D}^0(t)\rangle = \frac{1}{2}\left[\bar{\mathcal{A}}(s_0, s_+) + \frac{p}{q}\mathcal{A}(s_0, s_+)\right]e_1(t) + \frac{1}{2}\left[\bar{\mathcal{A}}(s_0, s_+) - \frac{p}{q}\mathcal{A}(s_0, s_+)\right]e_2(t), \tag{2}$$

with $e_{1,2}(t) = \exp\{-i(m_{1,2} - i\Gamma_{1,2}/2)t\}$. In the limit of CP conservation ($p/q = 1$), Eqs. (1) and (2) simplify to

$$\langle K^0_S K^+ K^-|D^0(t)\rangle = \mathcal{A}_1(s_0, s_+)e_1(t) + \mathcal{A}_2(s_0, s_+)e_2(t) \tag{3}$$

$$\langle K_S^0 K^+ K^- | \bar{D}^0(t) \rangle = \mathcal{A}_1(s_0, s_+) e_1(t) - \mathcal{A}_2(s_0, s_+) e_2(t), \tag{4}$$

where $\mathcal{A}_1(s_0, s_+) = [\mathcal{A}(s_0, s_+) + \bar{\mathcal{A}}(s_0, s_+)]/2$ and $\mathcal{A}_2(s_0, s_+) = [\mathcal{A}(s_0, s_+) - \bar{\mathcal{A}}(s_0, s_+)]/2$. In the isobar model the amplitudes $\mathcal{A}$ and $\bar{\mathcal{A}}$ are written as the sum of intermediate decay channel amplitudes (subscript r) with the same final state, $\mathcal{A}(s_0, s_+) = \sum_r a_r e^{i\phi_r} \mathcal{A}_r(s_0, s_+)$ and $\bar{\mathcal{A}}(s_0, s_+) = \sum_r \bar{a}_r e^{i\bar{\phi}_r} \bar{\mathcal{A}}_r(s_0, s_+) = \sum_r a_r e^{i\phi_r} \mathcal{A}_r(s_0, s_-)$, where CP conservation in decay has been assumed in the final step. If r is a CP eigenstate, then $\mathcal{A}_r(s_0, s_-) = \pm \mathcal{A}_r(s_0, s_+)$, where the sign $+(-)$ holds for a CP-even (-odd) eigenstate. Hence the amplitude $\mathcal{A}_1$ is CP-even, and the amplitude $\mathcal{A}_2$ is CP-odd.

Upon squaring Eqs. (3) and (4) we obtain for the time-dependent decay rates of initially produced D^0 and $\bar{D}^0$

$$\frac{dN(s_0, s_+, t)}{dt} \propto |\mathcal{A}_1(s_0, s_+)|^2 e^{-(t/\tau)(1+y)} + |\mathcal{A}_2(s_0, s_+)|^2 e^{-(t/\tau)(1-y)} + 2\mathrm{Re}[\mathcal{A}_1(s_0, s_+)\mathcal{A}_2^*(s_0, s_+)] \cos\left(x\frac{t}{\tau}\right) e^{-(t/\tau)} + 2\mathrm{Im}[\mathcal{A}_1(s_0, s_+)\mathcal{A}_2^*(s_0, s_+)] \sin\left(x\frac{t}{\tau}\right) e^{-(t/\tau)} \tag{5}$$

$$\frac{d\bar{N}(s_0, s_+, t)}{dt} \propto |\mathcal{A}_1(s_0, s_+)|^2 e^{-(t/\tau)(1+y)} + |\mathcal{A}_2(s_0, s_+)|^2 e^{-(t/\tau)(1-y)} - 2\mathrm{Re}[\mathcal{A}_1(s_0, s_+)\mathcal{A}_2^*(s_0, s_+)] \cos\left(x\frac{t}{\tau}\right) e^{-(t/\tau)} - 2\mathrm{Im}[\mathcal{A}_1(s_0, s_+)\mathcal{A}_2^*(s_0, s_+)] \sin\left(x\frac{t}{\tau}\right) e^{-(t/\tau)}, \tag{6}$$

where $\tau = 1/\Gamma$ is the D^0 lifetime. It can be shown (see the Appendix) that in the projection of the Dalitz plot onto s_0, the last two terms in Eqs. (5) and (6) vanish. Hence, a projection onto s_0 of the time-dependent decay rate for $D^0 \to K_S^0 K^+ K^-$ in the limit of CP conservation depends only on the mixing parameter y:

$$\frac{dN(s_0, t)}{dt} \propto a_1(s_0) e^{-(t/\tau)(1+y)} + a_2(s_0) e^{-(t/\tau)(1-y)}, \tag{7}$$

where $a_{1,2}(s_0) = \int |\mathcal{A}_{1,2}(s_0, s_+)|^2 ds_+$.

Figure 1 shows the time-integrated projection of the decay rate [Eq. (7)] together with the $a_1(s_0)$ and $a_2(s_0)$ contributions; the plots are obtained using the Dalitz model of Ref. [14] and taking $y = 0$. The Dalitz model includes five CP-even intermediate states ($K_S^0 a_0(980)^0$, $K_S^0 f_0(1370)$, $K_S^0 f_2(1270)$, $K_S^0 a_0(1450)^0$, $K_S^0 f_0(980)$), one CP-odd intermediate state ($K_S^0 \phi(1020)$), and three flavor-specific intermediate states [$K^- a_0(980)^+$, $K^- a_0(1450)^+$, $K^+ a_0(980)^-$].

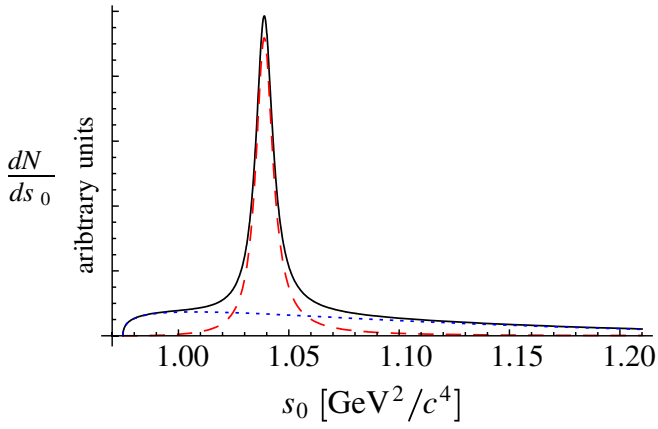

FIG. 1 (color online). Projection of time-integrated Dalitz distribution to s_0 (solid line), and the $a_1(s_0)$ (dotted line) and $a_2(s_0)$ (dashed line) contributions for the Dalitz model given in [14].

The two terms in Eq. (7) have a different time dependence as well as a different s_0 dependence (see Fig. 1). In any given s_0 interval, $\mathcal{R}$, and assuming $y \ll 1$, the effective D^0 lifetime is

$$\tau_{\mathcal{R}} = \tau[1 + (1 - 2f_{\mathcal{R}})y_{CP}], \tag{8}$$

where $f_{\mathcal{R}} = \int_{\mathcal{R}} a_1(s_0) ds_0 / \int_{\mathcal{R}} (a_1(s_0) + a_2(s_0)) ds_0$, which represents the effective fraction of the events in the interval $\mathcal{R}$ due to the $\mathcal{A}_1$ amplitude. In Eq. (8) we introduced the usual notation y_{CP} for the mixing parameter y to indicate that we assumed CP conservation in deriving Eq. (7). The definition of y_{CP} in Eq. (8) is consistent with that used in the $D^0 \to K^+K^-/\pi^+\pi^-$ measurement [4].

The mixing parameter y_{CP} can be determined from the relative difference in the effective lifetimes of the two s_0 intervals, one around the $\phi(1020)$ peak (interval ON) and the other in the sideband (interval OFF). Using Eq. (8) and taking into account the fact that $[1 - (f_{\mathrm{ON}} + f_{\mathrm{OFF}})]y_{CP} \ll 1$, we obtain

$$y_{CP} = \frac{1}{f_{\mathrm{ON}} - f_{\mathrm{OFF}}} \left(\frac{\tau_{\mathrm{OFF}} - \tau_{\mathrm{ON}}}{\tau_{\mathrm{OFF}} + \tau_{\mathrm{ON}}}\right). \tag{9}$$

The sizes of the ON and OFF intervals are chosen to minimize the statistical uncertainty on y_{CP}. They are determined using the Dalitz model of $D^0 \to K_S^0 K^+ K^-$ decays from Ref. [14]. The optimal intervals are found to be: $M_{K^+K^-} \in [1.015, 1.025]$ GeV/c^2 for the ON interval, and

the union of $M_{K^+K^-} \in [2m_{K^\pm}, 1.010]$ GeV/c^2 and $M_{K^+K^-} \in [1.033, 1.100]$ GeV/c^2 for the OFF interval.

III. MEASUREMENT

This section is organized as follows: in subsection III A we describe how signal decays are reconstructed; in subsection III B we describe how the mean decay time of the signal is extracted in the presence of background; in subsections III C and III Dwe describe how the background fraction and mean lifetime, respectively, are determined; in subsection III E we describe how $f_{\rm ON} - f_{\rm OFF}$ is determined; and in subsection III F we give the result for y_{CP}.

A. Reconstruction of events

The data were recorded with the Belle detector at the KEKB asymmetric-energy e^+e^- collider [15]. The Belle detector consists of a silicon vertex detector (SVD), a 50-layer central drift chamber (CDC), an array of aerogel threshold Cherenkov counters (ACC), a barrel-like arrangement of time-of-flight scintillation counters (TOF), and an electromagnetic calorimeter (ECL) comprised of CsI(Tl) crystals located inside a superconducting solenoid coil that provides a 1.5 T magnetic field. An iron flux-return located outside of the coil is instrumented to detect K_L^0 mesons and to identify muons (KLM). The detector is described in detail elsewhere [16]. Two inner detector configurations were used. A 2.0 cm beampipe and a 3-layer silicon vertex detector was used for the first sample of 156 fb^{-1}, while a 1.5 cm beampipe, a 4-layer silicon detector and a small-cell inner drift chamber were used to record the remaining 517 fb^{-1} of data [17]. We use an EVTGEN- [18] and GEANT-based [19] Monte Carlo (MC) simulated sample, in which the number of reconstructed events is about 3 times larger than in the data sample, to study the detector response.

The K_S^0 candidates are reconstructed in the $\pi^+\pi^-$ final state. We require that the pion candidates form a common vertex with a χ^2 fit probability of at least 10^{-3}, and that they be displaced from the e^+e^- interaction point (IP) by at least 0.9 mm in the plane perpendicular to the beam axis. We also require that they have an invariant mass $M_{\pi^+\pi^-}$ in the interval $[0.468, 0.526]$ GeV/c^2. We reconstruct D^0 candidates by combining the K_S^0 candidate with two oppositely charged tracks assumed to be kaons. We require charged kaon candidate tracks to satisfy particle identification criteria based upon dE/dx ionization energy loss in the CDC, time-of-flight, and Cherenkov light yield in the ACC [20]. These tracks are required to have at least one SVD hit in both $r-\phi$ and z coordinates. A D^0 momentum greater than 2.55 GeV/c in the e^+e^- center-of-mass frame is required to reject D mesons produced in B-meson decays and to suppress combinatorial background. Events with a $K_S^0K^+K^-$ invariant mass ($M_{K_S^0K^+K^-}$) in the interval $[1.77, 1.96]$ GeV/c^2 are retained for further analysis.

The proper decay time of the D^0 candidate is calculated by projecting the vector joining the production and decay vertices, $\vec{L}$, onto the D^0 momentum vector $\vec{p}_D$: $t = (m_{D^0}/p_D)\vec{L}\cdot(\vec{p}_D/p_D)$, where m_{D^0} is the nominal D^0 mass. Charged and neutral kaon candidates are required to originate from a common vertex for which the χ^2 fit probability is larger than 10^{-3}. According to simulation studies, if the D^0 decay position is determined by fitting the two prompt charged tracks to a common vertex, the decay length and the opening angle of the K^+ and K^- (and thus their invariant mass) are strongly correlated. This correlation is avoided by determining the D^0 decay length from a fit where only a single charged kaon and the K_S^0 are fitted to a common vertex. Both $K^\pm K_S^0$ vertex combinations are required to have a χ^2 probability larger than 10^{-3}; for the $\vec{L}$ determination, the one with the higher χ^2 fit probability is chosen. The D^0 production point is taken to be the intersection of the trajectory of the D^0 candidate with the IP region. The average position of the IP is calculated for every ten thousand events from the primary vertex distribution of hadronic events. The size of the IP region is typically 3.5 mm in the direction of the beam, 100 μm in the horizontal direction, and 5 μm in the vertical direction. The uncertainty in a D^0 candidate's proper decay time (σ_t) is evaluated from the corresponding covariance matrices. We require $\sigma_t < 600$ fs. The maximum of the σ_t distribution is at $\sim$230 fs.

Around 362×10^3 events pass all selection criteria. The $(M_{\pi^+\pi^-}, M_{K_S^0K^+K^-})$ and $M_{K^+K^-}$ distributions of these events are shown in Fig. 2.

B. Effective signal lifetime

We determine the effective lifetime of $D^0 \to K_S^0K^+K^-$ decays from the distribution of proper decay times as follows. The proper decay-time distribution of D^0 candidates can be parametrized as

$$\mathcal{P}(t) = p\frac{1}{\tau}\int e^{-t'/\tau}\cdot R(t-t', t_0)dt' + (1-p)B(t), \tag{10}$$

where the first term represents the measured distribution of signal events with lifetime τ, convolved with a resolution function, $R(t, t_0)$; t_0 corresponds to a possible shift of the resolution function from zero; $p = N_s/(N_s + N_b)$ is the fraction of signal events; and the last term, $B(t)$, describes the distribution of background events. Since the average of the convolution is the sum of the averages of the convolved functions, we can express the lifetime of signal events in region $\mathcal{R}$ (shifted for the resolution function offset) as

$$\tau_{\mathcal{R}} + t_0^{\mathcal{R}} = \frac{\langle t\rangle^{\mathcal{R}} - (1-p^{\mathcal{R}})\langle t\rangle_b^{\mathcal{R}}}{p^{\mathcal{R}}}, \tag{11}$$

where $\langle t\rangle^{\mathcal{R}}$ and $\langle t\rangle_b^{\mathcal{R}}$ are the mean proper decay times of all events and background events, respectively. By measuring

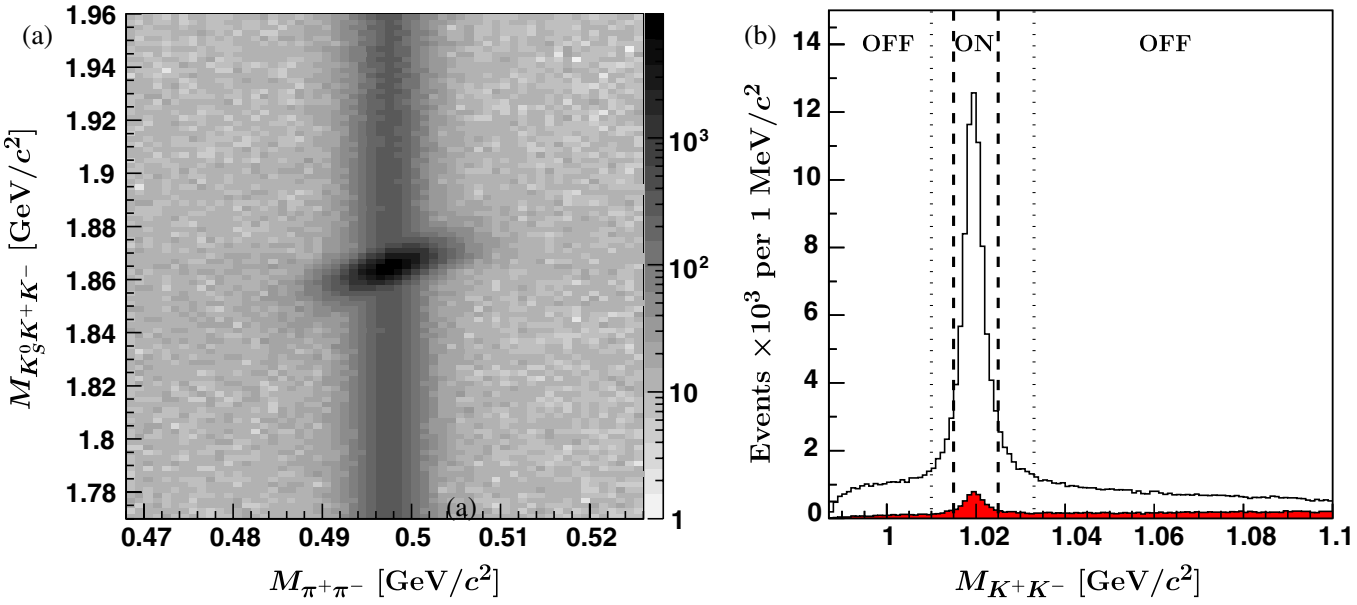

FIG. 2 (color online). (a) $(M_{\pi^+\pi^-}, M_{K^0_S K^+ K^-})$ distribution of selected events. (b) $M_{K^+K^-}$ distribution of events in the $|M_{K^0_S K^+ K^-} - m_{D^0}| < 10$ MeV/c^2 and $|M_{\pi^+\pi^-} - m_{K^0_S}| < 10$ MeV/c^2 region (unfilled histogram), and $20 < |M_{K^0_S K^+ K^-} - m_{D^0}| < 30$ MeV/c^2 and $|M_{\pi^+\pi^-} - m_{K^0_S}| < 10$ MeV/c^2 region (filled histogram). Dashed vertical lines indicate the boundaries of ON (OFF) intervals.

$\langle t \rangle^{\mathcal{R}}$ and $\langle t \rangle_b^{\mathcal{R}}$ for events in ON and OFF intervals of $M_{K^+K^-}$ we can obtain the two effective lifetimes and y_{CP} from Eq. (9). Note that the resolution function offset, t_0, if small ($t_0 \ll \tau$) and equal in ON and OFF regions, introduces a negligible bias ($\approx y_{CP} \cdot t_0/\tau$) in the measurement, since it cancels in the numerator of Eq. (9). We use the simulated sample to confirm that the resolution function offsets t_0^{ON} and t_0^{OFF} are equal to within the statistical uncertainty.

The requirement of minimal K^0_S candidate flight distance introduces a bias in the reconstructed mean proper decay time of signal $D^0 \to K^0_S K^+ K^-$ decays: events where both D^0 and K^0_S candidates are short-lived are rejected by this requirement. This introduces a $+0.5\%$ bias in the mean of the measured proper decay times for $D^0 \to K^0_S K^+ K^-$; the effect on the y_{CP} parameter is smaller and is included in the systematic error.

C. Signal and background fractions

Signal and background fractions are determined from a fit to the distribution of events in the $(M_{\pi^+\pi^-}, M_{K^0_S K^+ K^-})$ plane. In order to model the correlation between invariant masses $M_{K^0_S K^+ K^-}$ and $M_{\pi^+\pi^-}$ of signal events (see Fig. 2), we parametrize the signal shape by a rotated triple two-dimensional Gaussian distribution. The individual Gaussians are required to have the same mean value, which is allowed to vary in the fit. The ratio of the Gaussian widths is fixed to the MC simulated value, and only the width of the core Gaussian and the three correlation coefficients are left free.

Background events are classified into three categories according to their distribution in the $(M_{\pi^+\pi^-}, M_{K^0_S K^+ K^-})$ plane (see Fig. 2): true K^0_S background, $D^0 \to K^+K^-\pi^+\pi^-$ decays with the pion pair not originating from a K^0_S, and remaining background. True K^0_S background events are random combinations of charged kaons with correctly reconstructed K^0_S candidates; the shape in $M_{\pi^+\pi^-}$ is fixed to be the same as signal while in $M_{K^0_S K^+ K^-}$ it is parametrized with a second-degree polynomial. The remaining background events are random combinations of charged particles and are parametrized as a polynomial of first degree in $M_{\pi^+\pi^-}$ and second degree in $M_{K^0_S K^+ K^-}$. The $D^0 \to K^+K^-\pi^+\pi^-$ decays are peaking in $M_{K^0_S K^+ K^-}$, but not in $M_{\pi^+\pi^-}$. According to MC simulation, the contribution of these events is small ($\sim 0.1\%$); thus they are not included in the fit but considered as a systematic uncertainty.

The fractions and shapes are determined in a three-step fit for both ON and OFF regions. First, the fraction of signal events F_{sig} is obtained from a fit to the one-dimensional projection in $M_{K^0_S K^+ K^-}$. In the second step, we fit the projection in $M_{\pi^+\pi^-}$ to find the sum of the fractions of signal and true K^0_S (TKS) events, $F_{\mathrm{sig}} + F_{\mathrm{TKS}}$. Finally, we determine the signal shape parameters from a two-dimensional fit in which we use the F_{sig} and F_{TKS} results from the previous steps. The fitting procedure was checked using a high-statistics sample of simulated signal and background events and found to correctly reproduce the true event fractions.

The results of this procedure are shown in Fig. 3. We find $(72.3 \pm 0.4) \times 10^3$ signal events in the ON region and $(62.3 \pm 0.7) \times 10^3$ events in the OFF region. To achieve the best statistical accuracy on the y_{CP} measurement, we

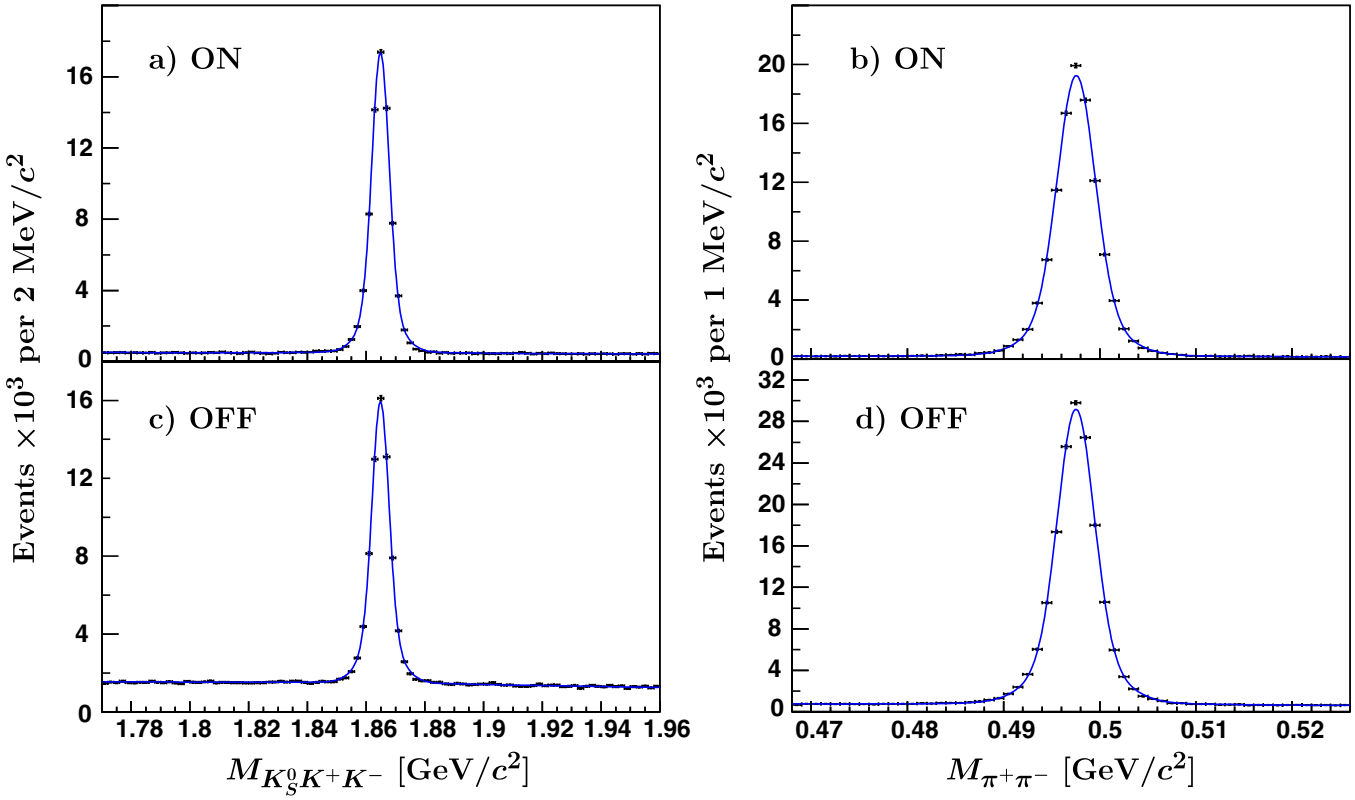

FIG. 3 (color online). Invariant masses $M_{K^0_S K^+ K^-}$ (a) and (c), and $M_{\pi^+\pi^-}$ (b) and (d) of events passing all selection criteria for ON and OFF intervals in $M_{K^+K^-}$. Superimposed on the data (points with error bars) are results of the fit (solid line).

optimize the size of the signal box. Because the invariant masses $M_{K^0_S K^+ K^-}$ and $M_{\pi^+\pi^-}$ are correlated for signal events, we define the signal box in the rotated variables:

$$\xi = \frac{M_{\pi^+\pi^-} - M_{K^0_S}}{\sigma_{K^0_S}} \tag{12}$$

$$\zeta = \frac{\rho}{\sqrt{1-\rho^2}}\xi - \frac{1}{\sqrt{1-\rho^2}}\frac{M_{K^0_S K^+ K^-} - M_{D^0}}{\sigma_{D^0}}, \tag{13}$$

where $M_{K^0_S} = 497.533 \pm 0.005$ MeV/c^2 and $M_{D^0} = 1864.874 \pm 0.009$ MeV/c^2 are fitted K^0_S and D^0 masses, $\sigma_{K^0_S} = 1.880 \pm 0.008$ MeV/c^2 and $\sigma_{D^0} = 2.839 \pm 0.014$ MeV/c^2 are widths of the core Gaussian function, and $\rho = 0.571 \pm 0.003$ is the correlation coefficient. The uncertainties are statistical only. The signal region that minimizes the statistical uncertainty on y_{CP} (signal box) is found to be $|\xi| < 3.9$ and $|\zeta| < 2.2$. The two-dimensional distribution of (ξ, ζ) for the selected data is shown in Fig. 4. The signal fractions in the signal box are $(96.94 \pm 0.06)\%$ and $(90.53 \pm 0.16)\%$ in the ON and OFF intervals, respectively.

The fraction of $D^0 \to K^+K^-\pi^+\pi^-$ decays in the signal box is estimated by fitting the $M_{K^0_S K^+ K^-}$ projection for events in the sideband regions $M_{\pi^+\pi^-} < 0.480$ GeV/c^2 and $M_{\pi^+\pi^-} > 0.514$ GeV/c^2, where the contributions of signal and true K^0_S background are small. The fractions of this background extrapolated to the signal box are found to be $(0.02 \pm 0.01)\%$ and $(0.07 \pm 0.02)\%$ in the ON and OFF intervals, respectively, and are reproduced well by MC simulation.

D. Mean proper decay time of background events

The mean proper decay time of background inside the signal box, $\langle t \rangle_b$, is determined from sideband regions A and B in the (ξ, ζ) plane as shown in Fig. 4. The regions are chosen larger than the signal box to minimize the uncertainty on $\langle t \rangle_b$. To an excellent approximation, the mean proper decay times in sideband regions A and B ($\langle t \rangle^A$ and $\langle t \rangle^B$) can be expressed as

$$\langle t \rangle^A = p^A_{\rm TKS}\langle t \rangle_{\rm TKS} + p^A_{\rm rest}\langle t \rangle_{\rm rest}, \tag{14}$$

$$\langle t \rangle^B = p^B_{\rm TKS}\langle t \rangle_{\rm TKS} + p^B_{\rm rest}\langle t \rangle_{\rm rest}, \tag{15}$$

where $p^{A(B)}_{\rm TKS}$ and $p^{A(B)}_{\rm rest}$ are the fractions of true K^0_S and the remaining background in region $A(B)$. Similarly, the mean proper decay time of background in the signal box S can be expressed as

$$\langle t \rangle_b = p^S_{\rm TKS}\langle t \rangle_{\rm TKS} + p^S_{\rm rest}\langle t \rangle_{\rm rest}. \tag{16}$$

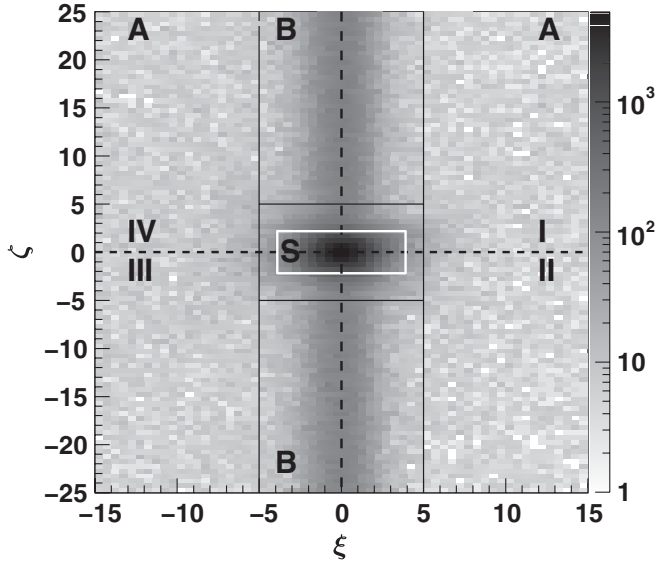

FIG. 4. The (ξ, ζ) distribution of selected events. Signal box S and sideband regions A and B are defined in the text. Quadrants denoted by I–IV are used in the systematic uncertainty estimate, as described in Sec. IV.

By solving Eqs. (14) and (15) for $\langle t\rangle_{\rm TKS}$ and $\langle t\rangle_{\rm rest}$, and inserting the results into Eq. (16), we obtain

$$\langle t\rangle_b = \frac{P^S(\langle t\rangle^A - \langle t\rangle^B) + P^A\langle t\rangle^B - P^B\langle t\rangle^A}{P^A - P^B}, \qquad (17)$$

where $P^i = p^i_{\rm TKS}/(p^i_{\rm TKS} + p^i_{\rm rest})$, $i = A, B, S$. The fractions $p^i_{\rm TKS}$ and $p^i_{\rm rest}$, $i = A, B, S$ are calculated from the results of the two-dimensional fit discussed in the previous section. In Table I we list the quantities used in Eq. (17) and the resulting $\langle t\rangle_b$ for regions ON and OFF.

In deriving Eq. (17), we have assumed that in regions A, B, and S the mean proper decay times $\langle t\rangle_{\rm TKS}$ and $\langle t\rangle_{\rm rest}$ are equal. This assumption has been validated using MC simulation. We have also neglected the signal leakage into regions A and B; if we compare, using MC simulation, the mean proper decay time of background events found in the signal box with that calculated from Eq. (17), we find agreement well within 1 standard deviation. The small deviations due to these assumptions are included in the systematic uncertainty.

E. Fit to the s_0 distribution

The $\mathcal{A}_1$ fractions, $f_{\rm ON}$ and $f_{\rm OFF}$, are obtained from a fit to the s_0 distribution. We use two different Dalitz models of $D^0 \to K^0_S K^+ K^-$ decays to parametrize the distribution: a four-resonance model from Ref. [21], and an eight-resonance model from Ref. [14]. The main sensitivity to y_{CP} arises from $K^0_S\phi(1020)$ and $K^0_S a_0(980)^0$ intermediate states, since the two have opposite CP eigenvalues. Because all resonance parameters cannot be determined from a one-dimensional fit, we fix the parameters of the resonances with smaller fit fractions using the amplitudes and phases from the corresponding model and world averages for masses and widths; we vary only the amplitudes of $K^0_S\phi(1020)$ and $K^- a_0(980)^+$ (four-resonance model) or the amplitudes of $K^0_S\phi(1020)$ and $K^- a_0(1450)^+$ (eight-resonance model), mass and width of the $\phi(1020)$, and the coupling constant g_{KK} of the Flatte parametrization of the $a_0(980)^0$.

The signal distribution is parametrized as

$$\mathcal{F}_s(s_0) = \varepsilon(s_0)\int \varepsilon(s_+)|\mathcal{A}_1(s_0, s_+) + \mathcal{A}_2(s_0, s_+)|^2 ds_+, \qquad (18)$$

where ε is the reconstruction efficiency determined from a sample of MC events in which the decay mode was generated according to phase space; the efficiency is found to be factorizable in the Dalitz variables s_0 and s_+. The background parametrization is obtained from the sideband region $5 < |\zeta| < 25$, where $|\xi| < 3.9$ corresponds to the signal region. A χ^2 test of the MC s_0 distributions of background events from the signal and sideband regions yields $\chi^2 = 88.9$ for 99 degrees of freedom; thus we conclude that the s_0 distribution of events taken from the sideband region satisfactorily describes the background distribution in the signal box.

Figure 5 shows fit results for the eight-resonance model, which we use to determine the fraction difference $f_{\rm ON} - f_{\rm OFF}$, since it provides a better description of the s_0 distribution. The reduced χ^2 is 1.28 for the eight-resonance model and 1.91 for the four-resonance model for 230 degrees of freedom. In Table II the fraction differences $f_{\rm ON} - f_{\rm OFF}$ are given for both Dalitz models. The left column lists the values calculated from the data in Refs. [14,21], and the

TABLE I. Mean proper decay times of events populating sideband regions A and B in the (ξ, ζ) plane, $\langle t\rangle^A$ and $\langle t\rangle^B$, fractions P^i $(i = S, A, B)$ and estimated mean proper decay times of background events, $\langle t\rangle_b$, populating the signal box, for events in the ON and OFF intervals in $M_{K^+K^-}$. The uncertainties are statistical only.

$M_{K^+K^-}$	$\langle t\rangle^A$ (fs)	$\langle t\rangle^B$ (fs)	P^S (%)	P^A (%)	P^B (%)	$\langle t\rangle_b$ (fs)
ON	223 ± 14	63.6 ± 4.7	93.31 ± 0.41	7.2 ± 1.8	91.83 ± 0.23	60.8 ± 4.8
OFF	237.7 ± 7.4	140.3 ± 3.1	90.17 ± 0.32	5.1 ± 1.2	88.02 ± 0.17	137.8 ± 3.2

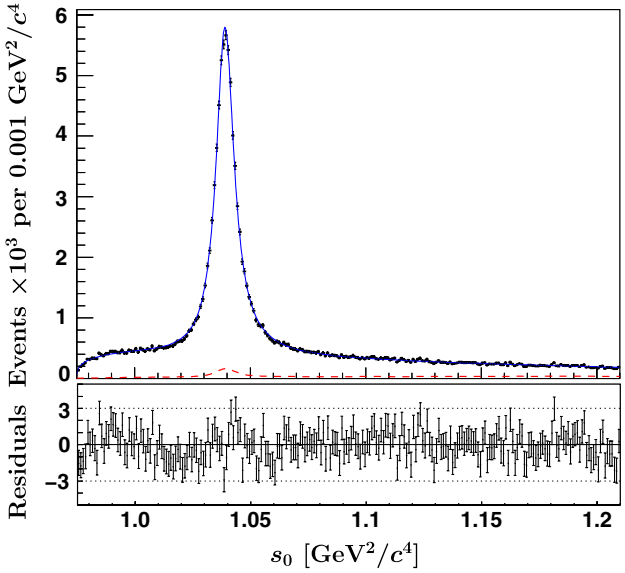

FIG. 5 (color online). The s_0 distribution of $D^0 \to K^0_S K^+ K^-$ decays with superimposed fit results for the eight-resonance Dalitz model given in Ref. [14]. The solid curve is the overall fitted function and the dashed curve represents the background contribution.

TABLE II. Fraction difference $f_{\rm ON} - f_{\rm OFF}$ for the two Dalitz models. The nominal values are calculated from the data in Refs. [14,21], and the fitted values from our fit results.

Model	$f_{\rm ON} - f_{\rm OFF}$ Nominal	Fitted
Four-resonance [21]	-0.730 ± 0.031	-0.732 ± 0.002
Eight-resonance [14]	-0.753 ± 0.004	-0.769 ± 0.005

right column lists the values calculated from the results of our fit. Uncertainties in $f_{\rm ON} - f_{\rm OFF}$ are calculated using the statistical errors of amplitudes and phases, without taking into account any correlation between them. Although the models are different, with distinct resonant structure [22], the differences $f_{\rm ON} - f_{\rm OFF}$ calculated for the two models are very similar. The small difference between them is included as a systematic uncertainty.

F. Results

Figure 6 shows the proper decay-time distributions of selected events in the signal box S for the ON and OFF intervals. The distribution of background events is estimated from proper decay-time distributions of events populating the sideband regions A and B and the known fractions of the true K^0_S background and the remaining background in all three regions. Inserting the values for $\langle t \rangle$, $\langle t \rangle_b$, and p (the fraction of signal) into Eq. (11) yields $\tau_{\rm ON} + t_0^{\rm ON} = (413.4 \pm 2.5)$ fs and $\tau_{\rm OFF} + t_0^{\rm OFF} = (412.7 \pm 3.0)$ fs. These results are summarized in Table III. The measured values for $\tau + t_0$ are close to the world average for τ_{D^0} and, since $y_{CP} \ll 1$, this implies t_0/τ is $\sim 1\%$ or less. Since the topology of events in the ON and OFF intervals is almost identical, we assume $t_0^{\rm ON} = t_0^{\rm OFF}$ and include a systematic error to account for possible deviations from this assumption. This leads to a normalized lifetime difference $(\tau_{\rm OFF} - \tau_{\rm ON})/(\tau_{\rm OFF} + \tau_{\rm ON}) = (-0.09 \pm 0.47)\%$ between the two regions, where the uncertainty is statistical only. The difference in the $\mathcal{A}_1$ fraction corresponding to the eight-resonance model (see Table II) is $f_{\rm ON} - f_{\rm OFF} = (-0.769 \pm 0.005)$; therefore, from Eq. (9) we obtain $y_{CP} = (+0.11 \pm 0.61(\text{stat.}))\%$.

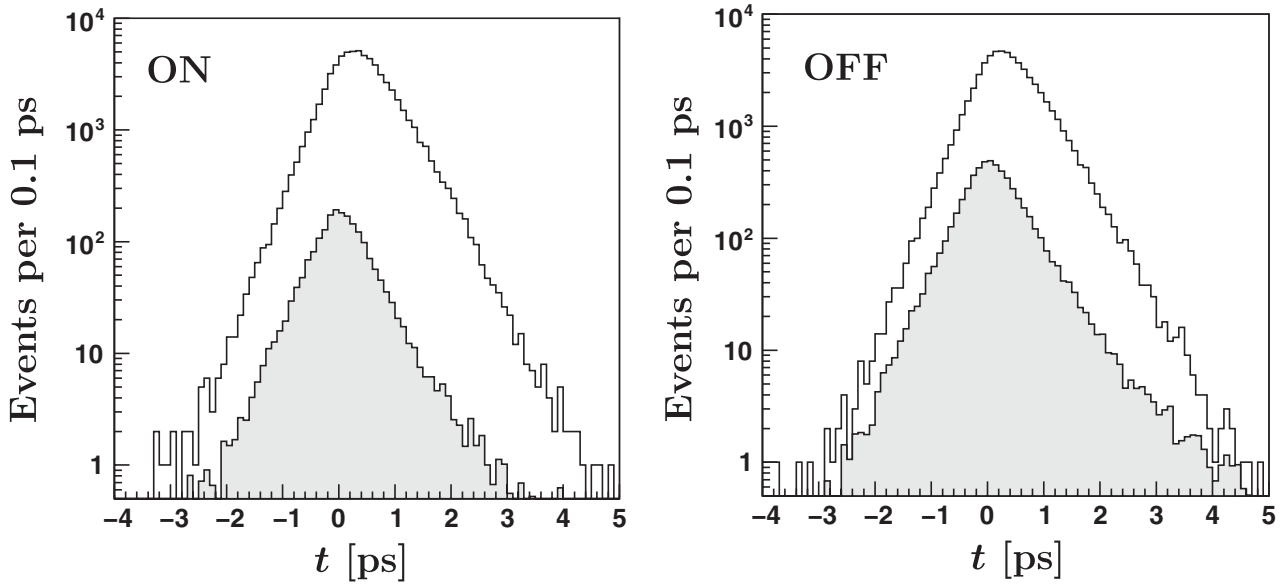

FIG. 6. The proper decay-time distributions of all events (unfilled histogram) and background events (hatched histogram) populating the signal box S for the ON and OFF intervals.

TABLE III. Measured mean proper decay times in the signal box $\langle t\rangle$, effective background lifetimes $\langle t\rangle_b$, signal fractions p, and the resulting effective signal lifetimes. The uncertainties are statistical only.

$M_{K^+K^-}$	$\langle t\rangle$ (fs)	$\langle t\rangle_b$ (fs)	p (%)	$\tau + t_0$ (fs)
ON	402.7 ± 2.5	60.8 ± 4.8	96.94 ± 0.06	413.4 ± 2.5
OFF	386.7 ± 2.6	137.8 ± 3.2	90.53 ± 0.16	412.7 ± 3.0

IV. SYSTEMATICS

We consider separately systematic uncertainties arising from experimental sources and from the $D^0 \to K^0_S K^+ K^-$ decay model. First, we check the simulated sample to confirm that the resolution function offsets $t_0^{\rm ON}$ and $t_0^{\rm OFF}$ are equal. The small difference observed is consistent with the statistical error but conservatively propagated to y_{CP} and taken as a systematic uncertainty ($\pm$ 0.38%).

The mean proper decay time of background events populating the signal box [calculated from Eq. (17)] assumes a negligible contribution of signal events in sideband regions A and B, and also assumes equal mean proper decay times of the two background categories in all three regions, A, B, and S. The systematic uncertainty resulting from the first assumption is evaluated by including the small residual fraction of signal events in regions A and B in the $\langle t\rangle_b$ calculation; the resulting change in y_{CP} is $\pm 0.01\%$. The uncertainty resulting from the second assumption is evaluated by MC simulation; mean proper decay times of the two background categories are found to be consistent within statistical uncertainty in all three regions. Small differences between the mean proper decay times of the two background categories in the S, A, and B regions result in $\pm 0.09\%$ and 0.04% variations of y_{CP} for true K^0_S and remaining background, respectively. We add in quadrature the above three contributions to obtain a $\pm 0.10\%$ systematic error on y_{CP}.

The contribution of $D^0 \to K^+K^-\pi^+\pi^-$ decays in our sample is found to be small and thus is not included. We evaluate their effect on y_{CP} by taking the fraction of these events in the ON and OFF intervals from data, and their mean proper decay time from the simulated sample. The resulting change in y_{CP} is $\pm 0.07\%$. We include this change in the systematic uncertainty.

We study the choice of sideband regions used to determine $\langle t\rangle_b$ as follows. The sidebands A and B are divided into four subregions (denoted I–IV) as shown in Fig. 4. The mean proper decay time of background events is then calculated using events in subregions (I, III) or (II, IV), and a difference of 0.05% in y_{CP} is observed. This change is included as a systematic uncertainty.

Possible systematic effects of selection criteria are studied by varying the signal box size and the selection criteria for σ_t and the K^0_S flight distance. Although no statistically significant deviation is observed, the maximum difference in y_{CP} is (conservatively) assigned as a systematic uncertainty ($\pm$ 0.30%).

The fitting procedure is tested using the simulated sample. A small difference between the fitted and true fractions of signal events in the signal box is propagated to y_{CP} and included as a systematic uncertainty ($\pm$ 0.10%).

The mean proper decay times of events populating the signal box S and the sideband regions A and B are taken to be the means of histograms of the proper decay times for events populating these regions. Changing the binning and intervals used in these histograms over a wide range results in a change in y_{CP} of $\pm 0.07\%$; we include this as an additional systematic uncertainty.

Finally, we estimate the systematic uncertainty due to our choice of $D^0 \to K^0_S K^+ K^-$ decay model. First, we compare the fraction difference $f_{\rm ON} - f_{\rm OFF}$ obtained using the four- and eight-resonance Dalitz models. Despite the difference between the models in their resonant substructure [22], the values for $f_{\rm ON} - f_{\rm OFF}$ are similar (see Table II). We assign a 3% relative error to y_{CP} due to the small difference in the above fractions. An additional 2% relative error is assigned due to the small difference between the fitted and nominal values of $f_{\rm ON} - f_{\rm OFF}$. If the reconstruction efficiency $\varepsilon(s_+)$ were constant, the contribution of the real and imaginary parts of the interference term $\mathcal{A}_1\mathcal{A}_2^*$ in Eq. (5) would vanish after integrating over s_+. A slight decrease of $\varepsilon(s_+)$ near the kinematic boundaries is observed from a large sample of simulated events; the effect of this variation on y_{CP} is studied and found to be negligible.

Adding all decay-model systematic uncertainties in quadrature with the statistical uncertainty in $f_{\rm ON} - f_{\rm OFF}$ ($= -0.769 \pm 0.005$; see Table II) yields a total uncertainty due to the decay model of 0.01%. Combining this in quadrature with all other sources of systematic uncertainty gives a total systematic error on y_{CP} of 0.52%. The individual contributions to the total systematic error are listed in Table IV.

TABLE IV. Sources of the systematic uncertainty on y_{CP}.

Source	Systematic error (%)
Resolution function offset difference $t_0^{\rm OFF} - t_0^{\rm ON}$	± 0.38
Estimation of $\langle t\rangle_b$	± 0.10
$D^0 \to K^+K^-\pi^+\pi^-$ background	± 0.07
Selection of sideband	± 0.05
Variation of selection criteria	± 0.30
Fitting procedure	± 0.10
Proper decay-time range and binning	± 0.07
Dalitz model	± 0.01
Total	± 0.52

V. SUMMARY

We present the first measurement of y_{CP} using a CP-odd final state in D^0 decays. Our method has the advantage of not requiring precise knowledge of the decay-time resolution function, and avoids several biases that can arise due to detector effects. The value of y_{CP} obtained is

$$y_{CP} = (+0.11 \pm 0.61(\text{stat.}) \pm 0.52(\text{syst.}))\%.$$

This measurement of y_{CP} using a CP-odd mode is consistent with previous measurements using CP-even final states [4,5], and with the world average value $y_{CP} = (+1.13 \pm 0.27)\%$ [9].

ACKNOWLEDGMENTS

We thank the KEKB group for the excellent operation of the accelerator, the KEK cryogenics group for the efficient operation of the solenoid, and the KEK computer group and the National Institute of Informatics for valuable computing and SINET3 network support. We acknowledge support from the Ministry of Education, Culture, Sports, Science, and Technology (MEXT) of Japan, the Japan Society for the Promotion of Science (JSPS), and the Tau-Lepton Physics Research Center of Nagoya University; the Australian Research Council and the Australian Department of Industry, Innovation, Science and Research; the National Natural Science Foundation of China under Contract Nos. 10575109, 10775142, 10875115, and 10825524; the Department of Science and Technology of India; the BK21 program of the Ministry of Education of Korea, the CHEP src program, and Basic Research program (Grant No. R01-2008-000-10477-0) of the Korea Science and Engineering Foundation; the Polish Ministry of Science and Higher Education; the Ministry of Education and Science of the Russian Federation and the Russian Federal Agency for Atomic Energy; the Slovenian Research Agency; the Swiss National Science Foundation; the National Science Council and the Ministry of Education of Taiwan; and the U.S. Department of Energy. This work is supported by a Grant-in-Aid from MEXT for Science Research in a Priority Area (''New Development of Flavor Physics''), and from JSPS for Creative Scientific Research (''Evolution of Tau-lepton Physics'').

APPENDIX: INTEGRATION OF $\mathcal{A}_1\mathcal{A}_2^*$ OVER ONE DALITZ VARIABLE

The amplitude $\mathcal{A}(\bar{\mathcal{A}})$ for a $D^0(\bar{D}^0)$ decay to a three-body final state, $h^+h^-m^0$, depends on invariant masses of all possible pairs of final state particles: $s_0 = M^2_{h^+h^-}$, $s_+ = M^2_{h^+m^0}$, and $s_- = M^2_{h^-m^0}$. Only two of these three are independent, since energy and momentum conservation results in a constraint

$$s_0 + s_+ + s_- = m^2_{D^0} + m^2_{h^+} + m^2_{h^-} + m^2_{m^0} \equiv m^2. \quad \text{(A1)}$$

In the limit of CP symmetry the following relation holds:

$$\bar{\mathcal{A}}(s_0, s_+) = \mathcal{A}(s_0, s_-) = \mathcal{A}(s_0, m^2 - s_+ - s_0), \quad \text{(A2)}$$

and amplitudes $\mathcal{A}_{1,2}$ (defined in Sec. II) are then

$$\mathcal{A}_1(s_0, s_+) = \frac{1}{2}[\mathcal{A}(s_0, s_+) + \mathcal{A}(s_0, m^2 - s_+ - s_0)], \quad \text{(A3)}$$

$$\mathcal{A}_2(s_0, s_+) = \frac{1}{2}[\mathcal{A}(s_0, s_+) - \mathcal{A}(s_0, m^2 - s_+ - s_0)]. \quad \text{(A4)}$$

We now show that

$$\int_{s_+^{\min}(s_0)}^{s_+^{\max}(s_0)} \mathcal{A}_1(s_0, s_+)\mathcal{A}_2^*(s_0, s_+)ds_+ = 0, \quad \text{(A5)}$$

where $s_+^{\min}(s_0)$ and $s_+^{\max}(s_0)$ are lower and upper bounds of Dalitz variable s_+. For a given value of s_0, the range of s_+ is determined by its values when the momentum of h^+ is parallel or antiparallel to the momentum of m^0:

$$s_+^{\max}(s_0) = (E^*_{h^+} + E^*_{m^0})^2 - (\sqrt{E^{*2}_{h^+} - m^2_{h^+}} - \sqrt{E^{*2}_{m^0} - m^2_{m^0}})^2, \quad \text{(A6)}$$

$$s_+^{\min}(s_0) = (E^*_{h^+} + E^*_{m^0})^2 - (\sqrt{E^{*2}_{h^+} - m^2_{h^+}} + \sqrt{E^{*2}_{m^0} - m^2_{m^0}})^2, \quad \text{(A7)}$$

where

$$E^*_{h^+} = \frac{s_0 + m^2_{h^+} - m^2_{h^-}}{2\sqrt{s_0}}, \quad \text{(A8)}$$

$$E^*_{m^0} = \frac{m^2_{D^0} - s_0 + m^2_{m^0}}{2\sqrt{s_0}} \quad \text{(A9)}$$

are the energies of h^+ and m^0 in the h^+h^- rest frame. The left-hand side of Eq. (A5) yields

$$I \equiv \int_{s_+^{\min}(s_0)}^{s_+^{\max}(s_0)} \mathcal{A}_1(s_0, s_+)\mathcal{A}_2^*(s_0, s_+)ds_+ = \frac{1}{4}(I_a - I_b + I_c - I_d), \quad \text{(A10)}$$

where

$$I_a = \int_{s_+^{\min}(s_0)}^{s_+^{\max}(s_0)} \mathcal{A}(s_0, s_+)\mathcal{A}^*(s_0, s_+)ds_+, \quad \text{(A11)}$$

$$I_b = \int_{s_+^{\min}(s_0)}^{s_+^{\max}(s_0)} \mathcal{A}(s_0, s_+)\mathcal{A}^*(s_0, m^2 - s_+ - s_0)ds_+, \quad \text{(A12)}$$

$$I_c = \int_{s_+^{\min}(s_0)}^{s_+^{\max}(s_0)} \mathcal{A}(s_0, m^2 - s_+ - s_0)\mathcal{A}^*(s_0, s_+)ds_+, \tag{A13}$$

$$I_d = \int_{s_+^{\min}(s_0)}^{s_+^{\max}(s_0)} \mathcal{A}(s_0, m^2 - s_+ - s_0)\mathcal{A}^*(s_0, m^2 - s_+ - s_0)ds_+. \tag{A14}$$

In integrals I_c and I_d we perform a variable substitution $s_+ \to s_-$ [Eq. (A1)]:

$$ds_+ = -ds_-, \tag{A15a}$$

$$s_+^{\max}(s_0) \overset{m_{h^+}=m_{h^-}}{\longrightarrow} s_+^{\min}(s_0), \tag{A15b}$$

$$s_+^{\min}(s_0) \overset{m_{h^+}=m_{h^-}}{\longrightarrow} s_+^{\max}(s_0), \tag{A15c}$$

and obtain

$$I_c = \int_{s_+^{\min}(s_0)}^{s_+^{\max}(s_0)} \mathcal{A}(s_0, s_-)\mathcal{A}^*(s_0, m^2 - s_- - s_0)ds_- = I_b, \tag{A16}$$

$$I_d = \int_{s_+^{\min}(s_0)}^{s_+^{\max}(s_0)} \mathcal{A}(s_0, s_-)\mathcal{A}^*(s_0, s_-)ds_- = I_a. \tag{A17}$$

The right-hand side of Eq. (A10) therefore yields zero.

[1] N. Cabibbo, Phys. Rev. Lett. **10**, 531 (1963); M. Kobayashi and T. Maskawa, Prog. Theor. Phys. **49**, 652 (1973).

[2] S. L. Glashow, J. Illiopoulos, and L. Maiani, Phys. Rev. D **2**, 1285 (1970).

[3] I. I. Bigi and N. Uraltsev, Nucl. Phys. **B592**, 92 (2001); A. F. Falk, Y. Grossman, Z. Ligeti, and A. A. Petrov, Phys. Rev. D **65**, 054034 (2002); A. F. Falk, Y. Grossman, Z. Ligeti, Y. Nir, and A. A. Petrov, Phys. Rev. D **69**, 114021 (2004).

[4] M. Staric *et al.* (Belle Collaboration), Phys. Rev. Lett. **98**, 211803 (2007).

[5] B. Aubert *et al.* (*BABAR* Collaboration), Phys. Rev. D **78**, 011105 (2008).

[6] B. Aubert *et al.* (*BABAR* Collaboration), Phys. Rev. Lett. **98**, 211802 (2007).

[7] T. Aaltonen *et al.* (CDF Collaboration), Phys. Rev. Lett. **100**, 121802 (2008).

[8] B. Aubert *et al.* (*BABAR* Collaboration), arXiv:0807.4544 [Phys. Rev. Lett. (to be published)].

[9] E. Barberio *et al.* (Heavy Flavor Averaging Group), arXiv:0808.1297.

[10] Throughout this paper, the inclusion of the charge-conjugate decay mode is implied unless stated otherwise.

[11] In the following, the nominal mass of particle X is denoted as m_X, while the reconstructed invariant mass of system Y is denoted as M_Y.

[12] L. M. Zhang *et al.* (Belle Collaboration), Phys. Rev. Lett. **99**, 131803 (2007).

[13] D. M. Asner *et al.* (CLEO Collaboration), Phys. Rev. D **72**, 012001 (2005).

[14] B. Aubert *et al.* (*BABAR* Collaboration), Phys. Rev. D **78**, 034023 (2008).

[15] S. Kurokawa and E. Kikutani, Nucl. Instrum. Methods Phys. Res., Sect. A **499**, 1 (2003), and other papers included in this volume.

[16] A. Abashian *et al.* (Belle Collaboration), Nucl. Instrum. Methods Phys. Res., Sect. A **479**, 117 (2002).

[17] Z. Natkaniec *et al.* (Belle SVD2 Group), Nucl. Instrum. Methods Phys. Res., Sect. A **560**, 1 (2006).

[18] D. J. Lange, Nucl. Instrum. Methods Phys. Res., Sect. A **462**, 152 (2001).

[19] R. Brun *et al.*, computer code GEANT 3.21, CERN Report No. DD/EE/84-1, 1984.

[20] E. Nakano, Nucl. Instrum. Methods Phys. Res., Sect. A **494**, 402 (2002).

[21] B. Aubert *et al.* (*BABAR* Collaboration), Phys. Rev. D **72**, 052008 (2005).

[22] In the Dalitz analysis of $D^0 \to K^0_S K^+ K^-$ decays [21], the Dalitz model includes the $K^0_S a_0(980)^0$, $K^0_S \phi(1020)$, $K^0_S f_0(1370)$, $K^0_S f_0(980)$, and $K^- a_0(980)^+$ contributions. The fitted fractions of the latter two are consistent with zero, and the authors do not quote their amplitudes and phases, so these two contributions are not used in this paper. In the Dalitz analysis of Ref. [14], the Dalitz model includes the $K^0_S a_0(980)^0$, $K^0_S \phi(1020)$, $K^0_S f_0(1370)$, $K^0_S f_2(1270)$, $K^0_S a_0(1450)^0$, $K^- a_0(980)^+$, $K^- a_0(1450)^+$, and $K^+ a_0(980)^-$ channels.